

# Distribution of the relaxation times of the new relaxor 0.4PSN-0.3PMN-0.3PZN ceramics

J. Macutkevic<sup>a</sup>, S. Lapinskas<sup>a</sup>, J. Grigas<sup>a</sup>, A. Brilingas<sup>a</sup>, J. Banys<sup>a</sup>, K. Meskonis<sup>a</sup>,  
K. Bormanis<sup>b</sup>, A. Sternberg<sup>b</sup>, and V. Zauls<sup>b</sup>

<sup>a</sup>*Faculty of Physics, Vilnius University, Sauletekio 9, 10222 Vilnius, Lithuania;*

<sup>b</sup>*Institute of Solid State Physics, University of Latvia, 8 Kengaraga str., 1063 Riga, Latvia*

**Abstract** The real distribution function of the relaxation times  $g(\tau)$  of the relaxor ferroelectric ceramics 0.4PSN-0.3PMN-0.3PZN is calculated from the experimental dielectric spectra obtained in the frequency range from 20 Hz to 1.25 GHz. Below the Burns temperature  $T_B \cong 380$  K, where the clusters begin to appear on cooling, the distribution of the relaxation times is symmetrically shaped. On cooling, the permittivity and loss spectra strongly broaden and slow down. The  $g(\tau)$  function becomes asymmetrically shaped and the second maximum appears. The width of the  $g(\tau)$  function is calculated at different temperatures. The shortest relaxation time is of the order of  $10^{-12}$  s and it remains almost temperature independent. The longest relaxation time diverges according to Vogel-Fulcher law.

**Keywords:** sintering, perovskites, dielectric properties.

## 1. Introduction

Since the discovery of relaxor ferroelectrics, a number of concepts have been introduced to account for their unusual physical behaviour: diffuse phase transition [1], superparaelectric [2] and dipolar glass models [3], random field frustrated ferroelectrics [4], and reorienting

polar clusters [5]. Recently, spherical random bond – random field model have been developed [6]. Nevertheless, the relaxors possess an extremely broad distribution of the relaxation times at low temperatures, which have not been fully understood. One of the latest attempts to explain such broad distribution has been made in [7]. A Landau type thermodynamic model based on the perovskite structure near the morphotropic phase boundary was proposed for calculating the energy barriers for polarization reversal near the polar cluster boundaries and due to that explaining the broad distribution of the relaxation times. It has been shown, that such broad distribution of the relaxation times at low temperatures is not attributed only to perovskite structures [8], and seems to be universal behaviour of disordered systems.

Recently, new ternary relaxor compounds  $\text{PbSc}_{1/2}\text{Nb}_{1/2}\text{O}_3$ - $\text{PbZn}_{1/3}\text{Nb}_{2/3}\text{O}_3$ - $\text{PbMg}_{1/3}\text{Nb}_{2/3}\text{O}_3$  (PSN-PZN-PMN) have been synthesized [9]. First dielectric investigations showed high value of dielectric permittivity (more than 10000 at  $T_{\text{max}}$  at 1 MHz), and temperature behaviour of permittivity and dielectric loss were typical for relaxors.

The aim of the present work is to investigate dielectric dispersion of 0.4PSN-0.3PMN-0.3PZN relaxor ceramics, and to discuss the distribution of the relaxation times and their temperature dependence.

## 2. Experimental

The ternary PSN-PZN-PMN solid solution was synthesized by solid state reactions from high grade oxides  $\text{PbO}_2$ ,  $\text{Nb}_2\text{O}_5$ ,  $\text{MgO}$ ,  $\text{ZnO}$ ,  $\text{Sc}_2\text{O}_3$ . The primary ingredients were homogenized and grinded in agate ball mill for 8 hours in ethanol and dried at 250° C for 24 hours. The dried mixture was fired in platinum crucibles. To obtain sufficient homogeneous mixture of perovskite structure the synthesis was repeated three times: at first at 800° C, the second at

900 ° C, the third at 1000 ° C, 2 hours each. After each synthesis the mixture was grinded in agate ball mill in ethanol, dried at 250° C for 24 hours, and the phase composition was analysed by X-ray diffraction.

The dielectric studies were performed by a computer controlled LCR meter HP 4284A in the frequency range 20 Hz to 1 MHz, and by the coaxial (frequency range 1 MHz to 4 GHz) dielectric spectrometers [11]. At high frequencies, the complex permittivity  $\epsilon^*$  was calculated taking into account the inhomogeneous distribution of the microwave field in the sample [11]. All the measurements were performed on cooling with the rate of 0.1 K/min in the weak electric fields ( $E \leq 100$  mV/cm).

### 3. Results and discussion

The temperature dependences of the real ( $\epsilon'$ ) and imaginary ( $\epsilon''$ ) parts of the complex dielectric permittivity  $\epsilon^*(\omega) = \epsilon' - i\epsilon''$  at different frequencies for 0.4PSN-0.3PMN-0.3PZN ceramics show a typical relaxor behaviour from low frequencies to microwaves (fig.1). Similar behaviour has been observed in PLZT relaxor ceramics [10]. Several points are worth mentioning:

- (i) static permittivity of this ceramics is very high, the peak value reaches 17,000 at frequencies lower than 0.1 kHz.
- (ii) the present results show typical relaxor behaviour in a very wide frequency range, from low frequencies to microwaves, and the peaks of  $\epsilon'$  and  $\epsilon''$  move towards higher temperatures with increasing frequency.
- (iii) permittivity remains of the order of 1,000 even in microwave range and losses are also very high ( $\tan \delta \geq 1$ ) at microwaves. It indicates that the main dielectric dispersion occurs in

the microwave range. Temperature-frequency dependence of the real and imaginary part of the permittivity shows a typical relaxational dispersion.

Near the temperature of the maximum permittivity,  $T_m$  the dispersion begins in the kilohertz region, but at higher temperatures the dispersion occurs in the higher frequency range of  $10^7$  to  $10^{11}$  Hz like in most of order-disorder ferroelectrics [11].

### 3.1. Analysis of the dielectric spectra

Owing to the roughly symmetrical shape of the Cole-Cole plots at high temperatures, the diffused dielectric spectra of 0.4PSN-0.3PMN-0.3PZN can be fitted by the empirical Cole-Cole equation:

$$\varepsilon^*(\omega) = \varepsilon_\infty + \frac{\Delta\varepsilon}{1 + (i\omega\tau)^\alpha}, \quad (1)$$

where  $\Delta\varepsilon = \varepsilon(0) - \varepsilon_\infty$ ,  $\Delta\varepsilon$  is the contribution of the relaxation to the static permittivity  $\varepsilon(0)$  (dielectric strength),  $\varepsilon_\infty$  is the contribution of the phonon modes and higher-frequency electronic processes to permittivity,  $\omega = 2\pi f$  is the angular frequency and  $\tau_0$  is the mean relaxation time. The parameter  $0 \leq \alpha \leq 1$  characterizes the distribution of relaxation times.

We have fitted the experimental Cole-Cole plots at different temperatures with equation (1) and determined the fitting parameters  $\varepsilon(0)$ ,  $\varepsilon_\infty$ ,  $\Delta\varepsilon$ ,  $\tau$  and  $\alpha$ . The almost temperature independent value  $\varepsilon_\infty \approx 40$  corresponds to the contribution of phonon modes. Temperature dependences of the fitted parameters  $\tau_0$  and  $\alpha$  are shown in figure 2. Cole-Cole fits were performed only in the limited temperature interval where the fits are reliable. At high temperatures, the relaxation frequencies approach the phonon soft mode, which is above the investigated frequency range.

At low temperatures (below 275 K),  $\varepsilon''$  is almost frequency independent, the dielectric spectrum is very diffused and a very wide distribution of relaxation times have been observed.

Frequency independence of  $\epsilon''$  does not allow estimating the relaxation time using conventional relaxation models or empirical equations. Therefore the low temperature dielectric spectra of 0.4PSN-0.3PMN-0.3PZN must be analysed separately.

The rapid increase in the mean relaxation time  $\tau$  with the temperature decrease (about 1000 times in the interval of 80 K - see figure 2) shows a substantial slowing down of the relaxation processes. The simultaneous increase in the distribution parameter  $\alpha$  up to the value of about  $\sim 0.9$  shows that the dielectric spectrum becomes extremely diffused. Correspondingly, the distribution of the relaxation times becomes extremely wide.

### 3.2. Uniform distribution function of the relaxation times

The diffused dielectric spectrum at low temperatures does not allow proper estimating the relaxation time using conventional relaxation models or empirical equations. A special algorithm was developed to resolve this problem.

The original program performs the direct calculation of relaxation time distribution function  $g(\tau)$  of the complex dielectric permittivity at fixed temperatures vs. frequency dependence according to superposition of the Debye-like processes:

$$\epsilon'(\nu) = \epsilon_{\infty} + \int_0^{\infty} \frac{g(\tau)}{1 + (2\pi\nu\tau)^2} d(\ln\tau), \quad \epsilon''(\nu) = \int_0^{\infty} \frac{2\pi\nu\tau g(\tau)}{1 + (2\pi\nu\tau)^2} d(\ln\tau). \quad (2)$$

The high-frequency limiting value  $\epsilon_{\infty}$  and the total contribution of the dipoles to the permittivity  $\Delta\epsilon = \int g(\tau) d(\ln\tau)$  can be either given together with the initial data or defined during the solution. This constrained regularized minimization problem is solved by least squares technique making use the simplified version of CONTIN program developed by Prowentcher [12] and later developed for dielectric spectra [13].

The real distribution function of the relaxation times of the 0.4PSN-0.3PMN-0.3PZN ceramics calculated from the experimental dielectric results (fig.1) is shown on figure 3. The

regularization parameter  $\alpha=5$  was found as optimal. Below the Burns temperature  $T_B \cong 380$  K, where the clusters begin to appear on cooling, the distribution of the relaxation times is symmetrically shaped (Cole-Cole function is satisfactory to describe the dielectric response). At lower temperatures, the distribution of the relaxation times becomes asymmetrically shaped. On further cooling the second maximum appears. With the decrease of the temperature it broadens to the long relaxation times and indicates a strong increase in inter-cluster correlation. Also, its contribution to the permittivity augments at lower temperatures.

The limits of the  $g(\tau)$  function were calculated (level 0.05 was chosen as sufficient accurate) at different temperatures (fig. 4). The shortest relaxation time is about  $10^{-12}$  s and it decreases slowly with the decrease of temperature. The spectra are compatible with the Jonscher's universal law [15]. The longest relaxation time diverge according to the Vogel-Fulcher law  $\tau = \tau_0 \exp(U_{VF}/[T - T_0])$ . The saturation of the  $g(\tau)$  function is caused by the finite lower frequency of experimental technique (reliable data were used from 100 Hz). The real distribution of the relaxation times gives the same freezing temperature,  $T_0 = 210$  K, but the activation energies are different,  $U_{VF} = E/k = 700$  K and 1000 K for Cole – Cole model and the real distribution function, respectively. These values are a little bit lower than in PLZT relaxor ceramics [10, 14].

Figure 5 shows the fits of the experimental dielectric spectrum with the relaxation times obtained from the uniform distribution function. The relaxation times describe well the experimental findings.

Broad dielectric spectra below room temperature indicate a strong increase in inter-cluster correlation. The low-frequency cut-off is much below 20 Hz (our lowest measured frequency) and the losses become independent of frequency. Appreciably high and temperature dependent losses and permittivity dispersion were observed also below  $T_0$  in the

nonergodic frozen phase. The quantitative estimate indicates a strongly anharmonic potential for polarization fluctuations which are restricted to inter-cluster boundaries.

## 5. Conclusions

On cooling, the dielectric dispersion and loss spectra of 0.4PSN-0.3PMN-0.3PZN relaxor ceramics strongly broaden and slow down. As they remain symmetric one can apply the Cole-Cole model and to determine the width of the uniform distribution function of the relaxation times and its temperature dependence above room temperature. The longest and mean relaxation times diverge according to the Vogel-Fulcher law with the same freezing temperature  $T_0 \cong 210$  K. The shortest relaxation time is about  $10^{-12}$  s and remains almost temperature independent. The spectra are compatible with the Jonscher's universal law. They broadening indicate a strong increase in inter-cluster correlation. The extraction of continuous relaxation times distribution of the Debye fundamental processes directly from the broadband dielectric spectra allows better understanding dynamic phenomena in solid state.

## References

1. Smolenski, G.A. & Isupov, V.A., Ferroelectric properties of solid solutions of barium tin in barium titanate. *Zhurnal tehnikeskoj Fiziki*, 1954, **24**, 1375–1386.
2. Cross, L.E., Relaxor ferroelectrics: an overview. *Ferroelectrics* 1994, **151**, 305-320.
3. Viehland, D., Jang, S.J., Cross, L.E. & Wuttig, M., Internal strain relaxation and the glassy behaviour of La – modified lead zirconate titanate relaxors. *J.Appl.Phys.*, 1991, 69, 6595-6602.

4. Viehland, D., Kleemann, W. & Glinchuk, M.D., Diffuse phase transitions and random-field-induced domain states of the "relaxor" ferroelectric  $\text{PbMg}_{1/3}\text{Nb}_{2/3}\text{O}_3$ . *Phys.Rev.Lett.*, 1992, **68**, 847-850.
5. Vugmeister, E. & Rabitz, H., Dynamics of interacting clusters and dielectric response in relaxor ferroelectrics. *Phys.Rev.B*, 1998, **57**, 7581-7585.
6. Pirc, R. & Blinc, R., Spherical random-bond-random-field model of relaxor ferroelectrics. *Phys.Rev.B*, 1999, **60**, 13470-13478.
7. Rychetsky, I., Kamba, S., Porokhonsky, V., Pashkin, A., Savinov, M., Bovtun, V., Petzelt, J., Kosec, M. & Dressel, M. Frequency independent dielectric losses ( $1/f$  noise) in PLZT relaxors at low temperatures. *J. Phys.: Condens. Matter*, 2003, **15**, 6017-6030.
8. Kamba, S., Porokhonsky, V., Pashkin, A., Bovtun, V. & Petzelt, J. Anomalous broad dielectric relaxation in  $\text{Bi}_{1.5}\text{Zn}_{1.0}\text{Nb}_{1.5}\text{O}_7$  pyrochlore. *Phys.Rev.B*, 2002, **66**, 054106.
9. Dambekalne, M., Bormanis, K., Sternberg, A. & Brante, I. Relaxor ferroelectric  $\text{PbSc}_{1/2}\text{Nb}_{1/2}\text{O}_3$ - $\text{PbZn}_{1/3}\text{Nb}_{2/3}\text{O}_3$ - $\text{PbMg}_{1/3}\text{Nb}_{2/3}\text{O}_3$  ceramics. *Ferroelectrics*, 2000, **240**, 221-228.
10. Kamba, S., Bovtun, V., Petzelt, J., Rychetsky, I., Mizaras, R., Brilingas, A., Banys, J., Grigas, J. & Kosec, M. Dielectric dispersion of the relaxor PLZT ceramics in the frequency range 20 Hz – 100 THz. *J. Phys.: Condens. Matter*, 2000, **12**, 497-519.
11. Grigas, J., *Microwave Dielectric Spectroscopy of Ferroelectrics and Related Materials*, OPA Gordon and Breach, Amsterdam, 1996, pp. 17-165.
12. Provencher, S.W., A constrained regularization method for inverting data represented by linear algebraic or integral equations. *Comput. Phys. Commun.*, 1982, **27**, 213-227.
13. Banys, J., Lapinskas, S., Kajokas, A., Matulis, A., Klimm, C., Völkel, G., & Klöpperpieper, A. Dynamic dielectric susceptibility of the betaine phosphate (0.15) betaine phosphate (0.85) dipolar glass. *Phys.Rev.B*, 2002, **66**, 144113.



14. Kajokas, A., Matulis, A., Banyš, J., Mizaras, R., Brilingas, A. & Grigas, J. Dielectric dispersion and distribution of the relaxation times of the relaxor PLZT ceramics. *Ferroelectrics*, 2001, **257**, 69-74.
15. Jonscher, A.K., *Dielectric Relaxation in Solids*, Chelsea Dielectric Press, London, 1983, pp. 85-115.

**Figure captions and figures**

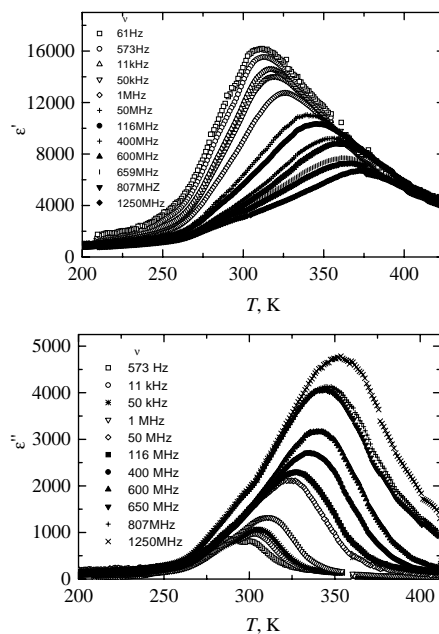


*Fig. 1.* Temperature dependence of real and imaginary parts of dielectric permittivity.

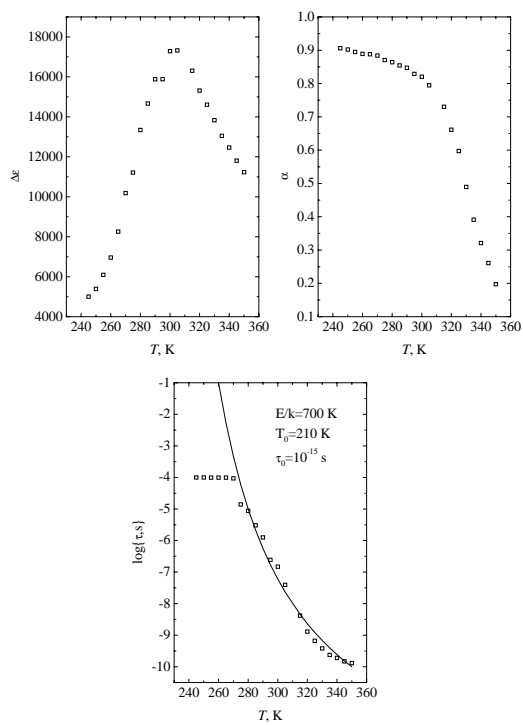


Fig.2. The fit parameters  $\Delta\epsilon$ ,  $\tau$  and  $\alpha$ .

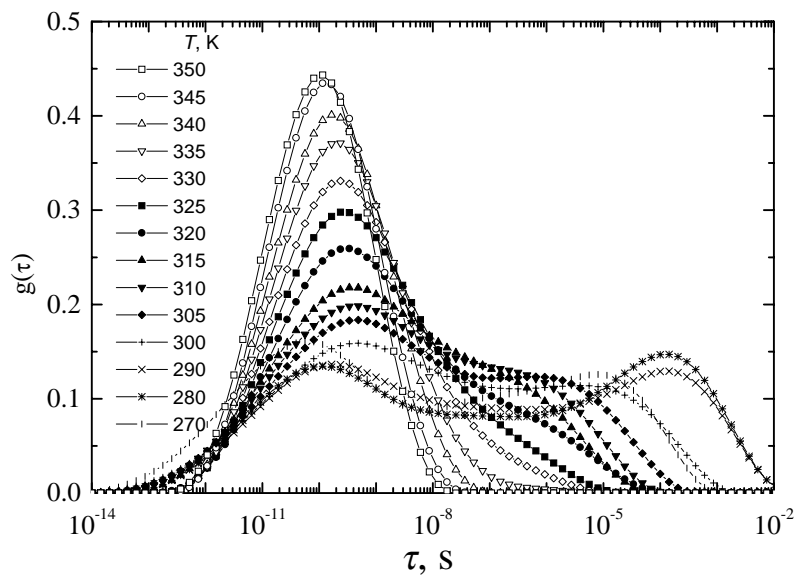


Fig.3. Distribution of the relaxation times.

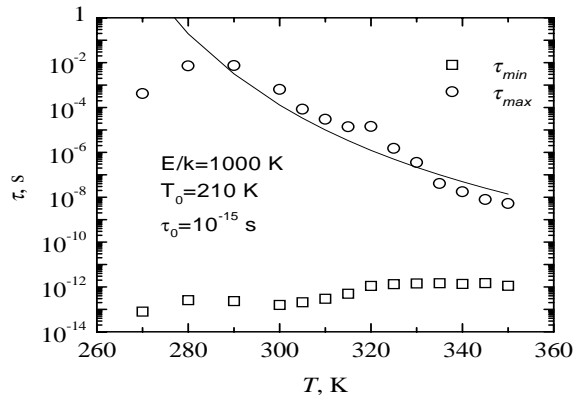
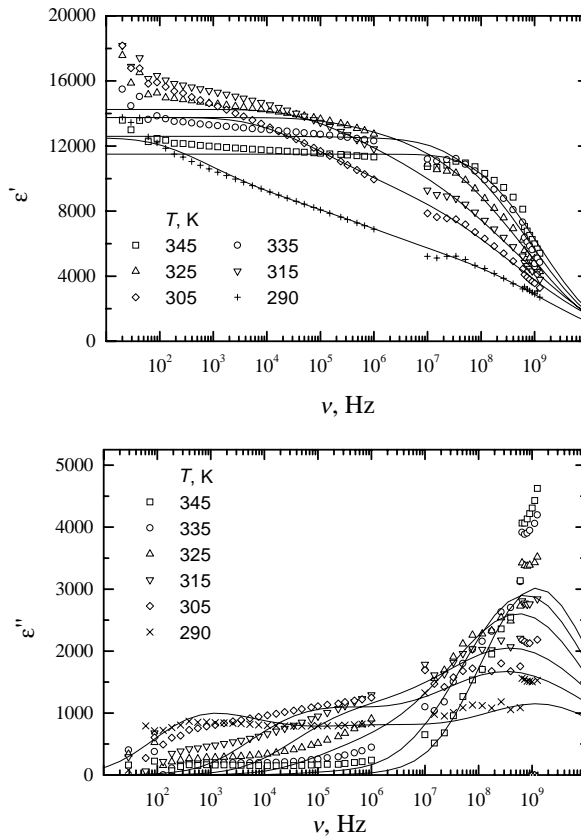


Fig. 4. Temperature dependence of upper and lower limits of relaxation time distribution.



*Fig. 5.* The best fits of real and imaginary parts of dielectric permittivity with uniform distributions of the relaxation times presented in fig.3.